

# 3D Point Cloud Based Spatio-Temporal Monitoring of Natural Objects

Jens-André PAFFENHOLZ, Germany, Bastian STEINHOFF-KNOPP, Germany and Corinna HARMENING, Austria

**Key words:** B-splines, Deformation measurement; Engineering survey; Laser scanning; Soil erosion

## SUMMARY

This paper deals with the research field of 3D point cloud based spatio-temporal monitoring focussed on natural objects. The 3D point clouds discussed here are predominantly acquired by means of laser scanners. The main characteristic of terrestrial laser scanners is their surface-based data acquisition, resulting in a 3D point cloud with typically millions of three-dimensional individual points along with at least intensity information and optional color information. This data allows for solving classical questions of monitoring and also to address new questions and monitoring applications, especially in the domain of natural, unstructured objects of different scales. Next to a literature review, starting from the challenges and new chances by the 3D point cloud based monitoring and showing exemplarily applications, we briefly introduce methods to approximate 3D point clouds with the aim to analyse soil erosion scenes. Afterwards, we highlight some results of self-conducted laboratory experiments to investigate soil erosion scenes with the focus on the quantification of soil erosion volumes. Therefore, we apply a GIS-based semi-automated identification of the soil erosion feature and its volume calculation. The aim of the approach presented here is to investigate the application of B-splines for the approximation of soil surfaces, and to identify methods and indicators with the potential to contribute to the process of fully automated volume determination of erosion features. Our results for the volume determination are compared with classical methods and show a promising correspondence.

# 3D Point Cloud Based Spatio-Temporal Monitoring of Natural Objects

**Jens-André PAFFENHOLZ, Germany, Bastian STEINHOFF-KNOPP, Germany and Corinna HARMENING, Austria**

## 1. MOTIVATION

This paper shows some new results of selected activities of the IAG working group (WG) 4.1.3 in collaboration with the FIG Commission 6 in the field of 3D point cloud based spatio-temporal monitoring. The focus of the IAG WG is on spatio-temporal monitoring of artificial and natural objects with the aid of 3D point clouds. Without loss of generality terrestrial laser scanners (TLS) are used to acquire 3D point clouds. The main characteristic of TLS is its surface-based data acquisition, resulting in a 3D point cloud with typically millions of three-dimensional individual points along with at least intensity information and optional color information. In addition to a high spatial resolution, a high temporal resolution with up to 1 million points per second is possible. TLS has proven to be a suitable technique for spatio-temporal monitoring of artificial structures like bridges, see e.g. Holst and Neuner (2021), Paffenholz and Wujanz (2019), Schill and Eichhorn, (2019) as well as of natural objects, see e. g. Butt et al. (2019), Holst et al. (2021), Harmening and Paffenholz (2021). Aforementioned authors show that the determination of object changes with high accuracy in the low millimeter level is feasible, see e. g., Wunderlich et al. (2016) for an overview. However, the use of TLS in the scope of geodetic monitoring tasks as an alternative to the classical point-wise deformation analysis is a highly topical research field, with several aspects currently being under investigation. These include for instance the establishment of an appropriate variance covariance matrix and the applied error model, e. g., Kermarrec et al. (2020) and Kerekes and Schwieger (2020), the deformation analysis itself, e. g. Harmening and Neuner (2020) and Mukupa et al. (2016), as well as the calibration of the sensors, e. g., Medić et al., (2020), to only mention a few aspects. Further challenges with respect to a laser scanning based deformation analysis arise due to the resulting high point density (Holst and Kuhlmann, 2016).

In engineering geodetic applications, the focus is usually on the monitoring of artificial objects, the laser scanner-based deformation analysis of which is already successfully conducted. However, laser scanning has also great potential with respect to the monitoring of natural objects and phenomena. Usually, further than the above mentioned challenges arise in natural environments. Using the volume determination of soil erosion scenes as an example, possibilities and difficulties of the laser scanner-based deformation analysis of natural objects are highlighted in this contribution.

The outline of the paper is as follows: Section 2 gives a comprehensive overview of the several contributions in literature in the scope of monitoring with the aid of 3D point clouds acquired by TLS sensors. Section 3 introduces our developed and applied methods. In Section 4, we utilize our proposed method to determine the volume of three erosion features. Finally, Section 5 concludes the paper and provides a perspective to future work.

## 2. STATE OF THE ART

In the scope of 3D point cloud based spatio-temporal monitoring a central question to answer first is: *How should 3D point clouds of different epochs be compared?* For instance, Mukupa et al. (2016) are addressing this question by giving three options. (1) Direct comparison of the original 3D point clouds of different epochs, i.e. point-to-point based comparison. (2) Compare an original 3D point cloud against a reference surface, i.e. point-to-surface comparison. The reference surface is obtained by modeling an original 3D point cloud, e. g., by a suitable surface approximation. (3) Make use of only models of 3D point clouds to obtain geometric object changes based on, i.e. surface-to-surface comparison. One of the major challenges is then the suitable modeling of the 3D point clouds (cf. Neuner et al. (2016) for a detailed overview of modeling strategies), as the objects under investigation typically vary in dimension and shape. In order to judge and to meaningful interpret changes and differences arising from the comparison of either two point clouds or two models of point clouds, the uncertainty budget of the sensor as well as the (geo-) referencing procedure and its uncertainty has to be taken into account. When analysing the uncertainty budget of the sensors, the focus is often on the range uncertainty (cf. e. g. Wujanz et al. (2017) and Winiwarter et al. (2020)). Alternatively, Kerekes and Schwieger (2020) apply the elementary error model to establish a variance covariance matrix, considering both range and angular uncertainties. Another approach to handle the sensor's uncertainties is the calibration of the laser scanner. Medić et al. (2020) report about the design and evaluation of a user-oriented calibration field for a target-based self-calibration of laser scanners. The (geo-) referencing procedure, which can be performed directly using additional sensors like GNSS equipment or indirectly using classical artificial targets, is discussed, e. g., in Osada et al. (2017), Paffenholz (2012) as well as Ugglá and Horemuz (2021). In the following, spatio-temporal monitoring based on 3D point clouds is reviewed for selected applications mainly coming from the infrastructure-building sector, and, hence, with the focus lying on artificial objects under investigation.

Liebig et al., (2011) discuss a combined application for structural measurements and 3D point clouds acquired by means of TLS sensors with the aim to calibrate a numerical model for a highway bridge under different traffic conditions. In particular, 3D point clouds for a static load scenario as well as 2D profiles in driving direction under various speed scenarios are acquired. The authors report about the ability to validate their numerical model, here a finite element model (FEM), by means of the 2D profiles acquired by means of the TLS.

Schill and Eichhorn (2019) use 2D profiles obtained by a TLS in order to monitor railway bridges. For two selected railway bridges, the authors demonstrate the benefits of TLS, being a non-contact measurement technique with a high spatial and high temporal resolution. This allows for the efficient capturing of temporally variable structural deformations, resulting in a considerably higher spatial resolution of the deformation information than it is provided by tactile sensors that are typically used for the deformation monitoring of bridge structures.

Truong-Hong and Lindenbergh (2019) deal with laser scanning-based monitoring of bridge structures, the deformations of which are due to increasing traffic load and aging structures. The authors introduce three approaches called point-to-surface (P2S), point-to-cell (P2C) and cell-to-cell (C2C) to describe the deformation of a structure by means of 3D point clouds. Furthermore, investigations about the impact of the selected reference surface or cell size on

the achieved accuracy of the deformation analysis are shown. As an example the authors present the task to measure the bridge's vertical clearance.

Eling (2009) reports about the structural monitoring of dams using a TLS sensor. The author splits his methodology into three parts (1) the deformation measurement and definition of a geodetic datum, (2) the 3D point cloud geo-referencing and (3) the analysis of the 3D point cloud using a voxel model and local filtering. The advantage is seen in a detailed spatial resolution of the structure, here a dam in Lower Saxony, Germany, and in the automation of the analysis.

Holst et al. (2015) introduce an approach for the area-based deformation analysis of a radio telescope's main reflector using a TLS. The authors emphasize the need for an appropriate measurement concept and for pre-processing steps, e. g., data reduction, object segmentation and sensor calibration, when making use of TLS in applications for deformation analysis.

Gojic et al. (2019) focus on the challenge to define point correspondences typically used in classical deformation analysis. The authors propose an algorithm establishing point-wise correspondences in the feature space utilizing a neural network based approach, which is also able to handle outliers. Their proposed algorithm outperforms traditional approaches in terms of obtaining true 3D displacement vectors.

The approximation process of 3D point clouds describing a complex freeform shell by means of B-spline surfaces is the topic of Schmitt et al. (2019). The authors point out the benefits of using 3D point clouds and their geometric approximation in the scope of the object's shape verification and its structural analysis. Furthermore, the interfacing between B-spline surfaces and FEM analysis is addressed.

The applications summarized above exclusively deal with the monitoring of artificial objects. However, laser scanning also offers great potential for monitoring natural objects and phenomena. Additional challenges usually arise in this case, which are closely related to the properties of the natural objects under investigation.

A typical example of the monitoring of natural objects in which laser scanning is increasingly used is phenotyping. Due to the advantages (automatic, contact-free and fast data acquisition) of laser scanners over sensors classically used in crop sciences, the use of laser scanning allows for the high throughput phenotyping that is required in plant sciences for achieving meaningful results. Hence, a number of approaches dealing with laser scanner-based phenotyping exist in literature (see e. g. Harmening and Paffenholz (2021), Jiang et al. (2019), Paulus (2019), Ziamtsov and Navlakha (2020)). Compared to the above described examples of the monitoring of artificial objects, in these applications great emphasis is usually placed on the development of appropriate segmentation strategies that automatically identify the plant organs of interest. Furthermore, the subsequent modelling of the segmented plant organs plays a prominent role, as simple geometric primitives, that are most often used to model artificial objects, are not appropriate.

As another example for the laser scanner-based monitoring of natural objects, which is also dealt with in this contribution, the monitoring of soil erosion scenes must be emphasized. In these applications, the determination of the soil erosion's volume is of superior importance. Usually this volume determination is not performed on the original 3D point clouds but on models of the 3D point clouds.

The basic and most common approach for the volume calculation of soil erosion features (rills, gullies, ephemeral gullies) is to calculate the difference of digital surface models (DSM) of two epochs (pre- and post-erosion). Applying this approach, e. g. Eltner et al. (2013, 2015) use multi-temporal UAV and TLS data to detect changes in the soil surface and estimate erosion loss.

Without information on the pre-erosion state, methods for reconstructing the original terrain surface are needed. This includes finding the ridge edge of erosion features. Addressing the development of an erosion gully in Spain, Marzloff and Poessen (2009) digitise the gully edge and calculate the volume change within the gully for three epochs, without calculating the volume of the whole gully. Implementing a similar approach, d'Oleire-Oltmanns et al. (2012) as well as Peter et al. (2014) monitor the volume of a gully by the means of UAV-derived DSMs. They use digitised 3D-lines of the gully edge to reconstruct the minimum terrain surface before the erosion occurred and calculate the difference between the surfaces to estimate the gully volume. Steinhoff-Knopp et al. (2019) use a comparable method to estimate the volume of small rills in a laboratory setting. Di Stefano et al. (2017) use structure from motion (SfM) techniques to generate a DSM of rills and extract cross sections to calculate the volume between the cross sections. Báčová et al. (2018) present an algorithm to determine the volume of erosion rills or gullies from DSMs and its implementation in the GIS software ArcGIS. By comparing their method within controlled conditions against results from the comparison of pre- and post-erosion surfaces (difference of surfaces), the authors estimate that their method underestimates the erosion volume by 10 – 15 %. Furthermore, the authors highlight the importance of identifying the ridge edge of the soil erosion feature to get valid results.

Our approach to determine the volume of soil erosion features is based on an adaption and refinement of the methods developed and applied by d'Oleire-Oltmanns et al. (2012), Báčová et al. (2018) and Steinhoff-Knopp et al. (2019). Hence, we start with a sophisticated pre-processing of the 3D point cloud by means of a B-spline approximation. Subsequently, we apply a GIS-based semi-automated identification of the soil erosion feature and its volume calculation. The aim of the approach presented here is to test the application of B-splines for the approximation of soil surfaces, and to identify methods and indicators with the potential to contribute to the process of fully automated volume determination of erosion features.

### 3. METHODS

#### B-spline surfaces

Free-form curves and surfaces have been used as part of a standard approximation method for 3D point clouds in many engineering disciplines in the past decade. Examples for geodetic applications can be found in Koch (2009), Harmening and Neuner (2015), Bureick et al. (2016), Paffenholz and Wujanz (2019) as well as Schmitt et al. (2019) who approximate captured 3D point clouds representing artificial objects by means of B-splines and non-uniform rational B-splines (NURBS). In addition, Harmening and Paffenholz (2021) use B-splines for the approximation of natural objects like plant leaves with the aim of leaf area determinations in phenotyping context. In this contribution, B-spline surfaces are used to approximate point clouds representing soil erosion features.

A B-spline surface of degree  $p$  and  $q$  is defined by:

$$\hat{S}(u, v) = \sum_{i=0}^{n_p} \sum_{j=0}^{m_p} N_{i,p}(u) \cdot N_{j,q}(v) \cdot P_{ij}$$

According to the previous equation, a surface point  $\hat{S}(u, v)$  is computed as the weighted average of the  $(n_p + 1) \times (m_p + 1)$  control points  $P_{ij}$  (Piegl and Tiller, 1997, p. 100). The corresponding weights are defined by the functional values of the B-spline basis functions  $N_{i,p}(u)$  and  $N_{j,q}(v)$ , which can be recursively computed (Cox, 1972; Boor, 1972). Two knot vectors, one in direction of the surface parameter  $u$  ( $U = [u_0, \dots, u_r]$ ) and one in direction of the surface parameter  $v$  ( $V = [v_0, \dots, v_s]$ ), split the B-spline's domain into knot spans.

Usually, only the location of the control points is estimated in a linear Gauß-Markov model when estimating a best-fitting B-spline surface. The choice of the optimal number of control points  $(n_p + 1)$  and  $(m_p + 1)$  to be estimated is a model selection problem and can be solved by classical model selection criteria or by structural risk minimisation (Harmening and Neuner, 2016; Harmening and Neuner, 2017). In order to obtain a linear relationship between the observations and the unknown control points  $P_{ij}$ , the B-spline's knots as well as its degrees are usually specified a priori. The use of cubic B-splines with  $p = q = 3$  is a commonly accepted choice. The determination of the knots (known as knot adjustment problem) considerably affects the estimation of the B-spline surface. Therefore, in Bureick et al. (2016) and Bureick et al. (2019) different approaches based on Monte Carlo techniques and genetic algorithms are developed with regard to B-spline curves. Both approaches show an optimal selection of knots for curve approximation. Finally, convenient surface parameters  $u$  and  $v$ , locating the observations on the surface to be estimated, have to be a-priori allocated to the observations (Harmening and Neuner, 2016).

Hence, the workflow for the B-spline approximation of a 3D point cloud can be briefly summarized as follows: (1) pre-processing of the 3D point cloud, (2) model selection and parametrization, (3) knot vector adjustment and (4) estimation of the B-spline surface in a linear Gauß-Markov model.

### GIS-based analysis of 3D point clouds with the aim of volume determination

To calculate the volume of soil erosion features utilizing 3D point clouds without knowledge of the pre-erosion surface, the following workflow is implemented by adapting approaches proposed by d'Oleire-Oltmanns et al. (2012), Báčová et al. (2018) and Steinhoff-Knopp et al. (2019). Our workflow is split in three parts, see Figure 1 for an exemplary visualization of relevant steps in the workflow. Namely the three parts are: A. the pre-processing of the original 3D point clouds, B. the semi-automated identification of the soil erosion feature and C. the volume calculation of the soil erosion feature. The parts B and C of the method are implemented in the software ArcGIS Pro 2.7.1 (ESRI 2020).

**Part A. Pre-Processing:** Use of an initial B-spline approximation of the acquired point clouds for the whole area of investigation. This leads to a smoothing effect of the noisy, original 3D point cloud (Figure 1 a). Also, it is an efficient way to systematically reduce the number of points, i.e., the point density, with respect to computational time in the analysis and moreover to apply the approach on large scale, real world data.

**Part B. Semi-automated identification of the soil erosion feature:** The steps in this part are as follows:

1. Conversion of B-spline approximated 3D point cloud to a raster representing the post-erosion soil surface. For this rasterization a regular grid resolution of 1 mm is chosen (Figure 1 b).
2. Cell-by-cell based calculation of the *local height deviation to the mean height of the area of interest*  $dev_z = \frac{z_i}{(\sum_k^m z_k) / n}$ , where  $z_i$  denotes the height value of raster cell  $i$ ,  $z_k$  denotes the height value of raster cell  $k$  and  $n$  represents the number of raster cells in the area of interest.
3. Selection of all raster cells with  $dev_z$ -values lower than the  $x$ . percentile, where  $x$  has to be defined at the moment by an analyst in a process of manual backward model selection. Calculations are conducted for each percentile ( $x = [1, 2, 3 \dots 100]$ ) as a basis for backward model selection. The criterion for the model selection is the agreement of the calculated volume with an externally determined volume of the soil erosion feature.
4. Extraction of all contiguous grid cells as regions of interest out of the selected raster cells (Figure 1 c).
5. Automatic selection of the largest region as the area of interest covering the relevant soil erosion feature and its conversion into a polygon (Figure 1 d).

**Part C. Volume calculation of the soil erosion feature:** The soil erosion feature volume calculation requires the following steps:

1. Usage of the edge of the previously generated polygon to extract the height / z-value of the soil surface at the edge of the soil erosion feature (Figure 1 e).
2. Creation of the reconstructed pre-erosion soil surface by triangulation of the z-values at the edge of the soil erosion feature (Figure 1 f).
3. Rasterization of the pre-erosion surface with a regular grid resolution of 1 mm.
4. Calculation of difference between post-erosion soil surface and reconstructed pre-erosion soil surface.

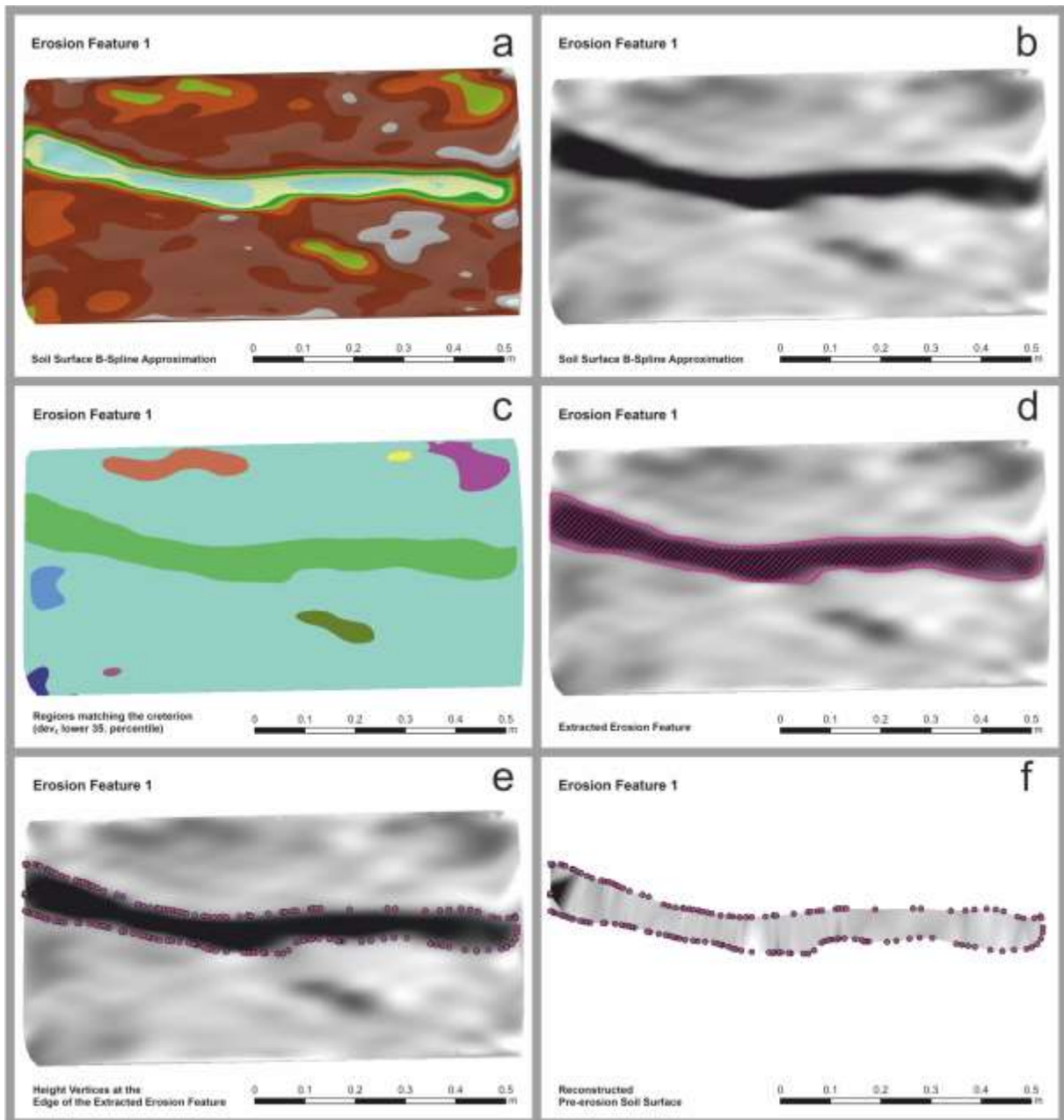


Figure 1: Visualisation of the workflow to identify the soil erosion feature and reconstruct the pre-erosion soil surface. Example for the erosion feature 1 (see Section 4).



#### 4. APPLICATION OF OUR PROPOSED METHOD TO THREE EROSION FEATURES

An experimental setup is chosen to develop and test the quantification method introduced in the previous section. For this purpose, three differently shaped erosion features (artificial rills) are created in a box filled with soil (see Figure 2, bottom).

The erosion features are captured with a terrestrial laser scanner of type Zoller+Fröhlich (Z+F) Imager 5010X with the acquisition parameters “resolution high” and “default noise”. To avoid shadowed areas, the 3D point clouds are captured from 8 fixed positions on each side and corner of the box (see Figure 2, top left). The individual 3D point clouds of each position are referenced via targets into a single 3D point cloud using the Z+F LaserControl software. This 3D point cloud serves as the basis for the subsequent determination of the erosion features’ volumes. Finally, the artificial erosion features are filled with quartz sand with a known density of 1.5 g/ml. The volumes determined by backweighting the quartz sand serve as reference and criterion for backward model selection (see Section 3) of the determined volumes.

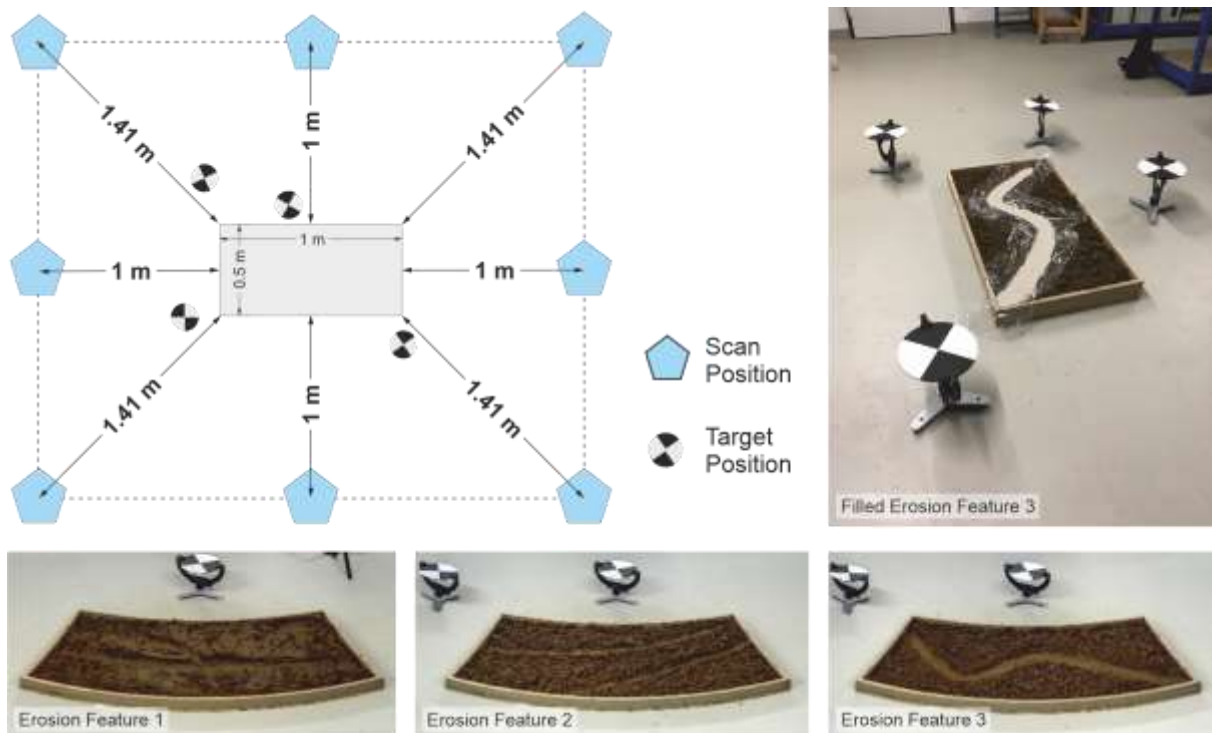


Figure 2: Design of the experimental setup: Position of the box filled with soil, the scan positions and targets (top left), pictures of the three evaluated erosion features (1, 2, 3, bottom), exemplary filling of erosion feature 3 with quartz sand for external volume determination (top right.)

Applying the method to determine the volume of the erosion features as described in Section 3, models are selected by backward model selection with the reference volume as selection

criterion. Table 1 summarises the results. It is possible to find satisfying fitting models for all three erosion features, with the applied percentile of  $dev_z$  varying from the 35. to the 56. percentile.

Table 1: Determined volumina of the soil erosion features and deviation to the external determined reference value.

Erosion Feature	Method	Volume [ml]	Deviation [%]
Erosion Feature 1	Filling with quartz sand (reference)	1927	-
	Semi-automatic GIS-based method (selected model: 43. percentile $dev_z$ )	1880	-2.44
Erosion Feature 2	Filling with quartz sand (reference)	960	-
	Semi-automatic GIS-based method (selected model: 35. percentile $dev_z$ )	961	0.10
Erosion Feature 3	Filling with quartz sand (reference)	1089	-
	Semi-automatic GIS-based method (selected model: 56. percentile $dev_z$ )	1078	-1.01

## 5. CONCLUSIONS AND OUTLOOK

This contribution aims to provide an overview of 3D point cloud based spatio-temporal monitoring. The literature review states that this research field is manifold and still under development with solved questions and challenges to tackle.

In particular, the huge amount of individual 3D points in the cloud, their proper approximation and finally the statistical testing of differences in the scope of a deformation analysis are current research topics. For statistical testing, the consideration of uncertainty information is mandatory. This can be seen as an independent research question and is approached, e.g., by (Wujanz et al., 2018).

In our ongoing research, we evaluated the quantification of soil erosion features by means of a TLS. The key challenge in this research is the quantification of soil loss volumes without knowledge about pre-erosion conditions. The method to calculate the volume of soil erosion features described here is capable of producing correct results in a process of stepwise backward modelling when an external reference is provided. Our results presented here also show that we have not yet found a generally valid parameter (resp. a value of a parameter) with which the determination of the volume can be automated. This reflects that the general approach has a high potential, but a parameter to automatise the selection of the erosion feature and reconstruct the pre-erosion soil surface is needed. Ongoing analysis of the data shows that such a parameter should take into account the roughness of the soil surface and the depth of the erosion form. A promising alternative approach to remodel the pre-erosion soil surface is to extract the ridge edge of the erosion feature.

## REFERENCES

- Báčová, M., Krása, J., Devátý, J., Kavka, P. (2019). A GIS method for volumetric assessments of erosion rills from digital surface models. *European Journal of Remote Sensing* 52 (sup1), 96–107. doi:10.1080/22797254.2018.1543556.
- Cox, M. G. (1972): The Numerical Evaluation of B -Splines. In: *IMA J Appl Math* 10 (2), S. 134–149. doi: 10.1093/imamat/10.2.134.
- Boor, C. de (1972): On calculating with B-splines. In: *Journal of Approximation Theory* 6 (1), S. 50–62. doi: 10.1016/0021-9045(72)90080-9.
- Bureick, J., Alkhatib, H., Neumann, I. (2019): Fast converging elitist genetic algorithm for knot adjustment in B-spline curve approximation. In: *Journal of Applied Geodesy* 13 (4), pp. 317–328. doi: 10.1515/jag-2018-0015.
- Bureick, J., Alkhatib, H., Neumann, I. (2016). Robust Spatial Approximation of Laser Scanner Point Clouds by Means of Free-form Curve Approaches in Deformation Analysis. In: *Journal of Applied Geodesy*, Vol. 10, No. 1, pp. 27–35, doi: 10.1515/jag-2015-0020.
- Butt, J.; Gojcic, Z.; Schmid, L.; Wieser, A. Terrestrische Radarinterferometrie und terrestrisches Laserscanning zur Überwachung alpinen Geländes: Praxiserfahrungen und Theorie. In: *Tagungsband GeoMonitoring 2020*. Braunschweig, S. 187-206. doi: 10.15488/9350.
- Di Stefano, C., Ferro, V., Palmeri, V., Pampalone, V. (2017). Measuring rill erosion using structure from motion: A plot experiment. *CATENA* 156, 383–392. doi:10.1016/j.catena.2017.04.023.
- d'Oleire-Oltmanns, S., Marzloff, I., Peter, K., Ries, J. (2012). Unmanned Aerial Vehicle (UAV) for Monitoring Soil Erosion in Morocco. *Remote Sensing* 4 (11), 3390–3416. doi:10.3390/rs4113390.
- Eling, D. (2009). *Terrestrisches Laserscanning für die Bauwerksüberwachung*. PhD thesis. Munich : DGK (Reihe C, 641).
- Eltner, A., Schneider, D., Maas, H.-G. (2016). Integrated Processing Of High Resolution Topographic Data For Soil Erosion Assessment Considering Data Acquisition Schemes And Surface Properties. *Int. Arch. Photogramm. Remote Sens. Spatial Inf. Sci. XLI-B5*, 813–819. doi:10.5194/isprs-archives-XLI-B5-813-2016.
- Eltner, A., Baumgart, P., Maas, H.-G., Faust, D. (2015). Multi-temporal UAV data for automatic measurement of rill and interrill erosion on loess soil. *Earth Surf. Process. Landforms* 40 (6), 741–755. doi:10.1002/esp.3673.
- ESRI Inc. (2020). *ArcGIS Pro (Release 2.7.1)*. Software. Redlands, USA
- Gojcic, Z., Zhou, C., Wieser, A (2019): Robust pointwise correspondences for point cloud based deformation monitoring of natural scenes. In: *Proceedings of the 4th Joint International Symposium on Deformation Monitoring (JISDM)*. Athens, Greece.
- Harmening, C., Neuner, H. (2020). A spatio-temporal deformation model for laser scanning point clouds. *Journal of Geodesy*, Vol. 94, doi:10.1007/s00190-020-01352-0.
- Harmening, C., Neuner, H. (2017). Choosing the optimal number of B-spline control points. Part 2: Approximation of surfaces and applications. In: *Journal of Applied Geodesy*, Vol. 11, No. 1, pp. 43–52, doi: 10.1515/jag-2016-0036.
- Harmening, C., Neuner, H. (2016). Choosing the optimal number of B-spline control points. Part 1: Methodology and Approximation of Curves. In: *Journal of Applied Geodesy*, Vol. 10, No. 3, pp. 139–157, doi: 10.1515/jag-2016-0003.
- Harmening, C., Neuner, H. (2015). A constraint-based parameterization technique for B-spline surfaces. In: *Journal of Applied Geodesy*, Vol. 9, No. 3, pp. 143–161, doi: 10.1515/jag-2015-0003.
- Harmening, C., Paffenholz, J.-A. (2021). A Fully Automated Three-Stage Procedure for Spatio-Temporal Leaf Segmentation with Regard to the B-Spline-Based Phenotyping of Cucumber Plants. *Remote Sens.* 2021, 13, 74, doi:10.3390/rs13010074.
- Jiang, Y., Li, C., Takeda, F., Kramer, E.A., Ashrafi, H., Hunter, J. (2019). 3D point cloud data to quantitatively characterize size and shape of shrub crops. *Hortic. Res.*, 6, 43, doi:10.1038/s41438-019-0123-9.

- Holst, C., Janßen, J., Schmitz, B., Blome, M., Dercks, M., Schoch-Baumann, A., Blöthe, J., Schrott, L., Kuhlmann, H., Medic, T. (2021). Increasing Spatio-Temporal Resolution for Monitoring Alpine Solifluction Using Terrestrial Laser Scanners and 3D Vector Fields. *Remote Sensing*, 13, 1192, doi:10.3390/rs13061192.
- Holst, C., Nothnagel, A., Blome, M., Becker, P., Eichborn, M., Kuhlmann, H. (2015). Improved area-based deformation analysis of a radio telescope's main reflector based on terrestrial laser scanning. In: *Journal of Applied Geodesy*, Vol. 9, No. 1, pp. 1–14, doi: 10.1515/jag-2014-0018 2015.
- Holst, C., Kuhlmann, H. (2016). Challenges and Present Fields of Action at Laser Scanner Based Deformation Analyses. In: *Journal of Applied Geodesy*, Vol. 10, No. 1, pp. 17–25, doi: 10.1515/jag-2015-0025.
- Holst, C., Neuner, H. (2021). Spatio-Temporal Models for Vibration Monitoring of Elongated Structures Using Profile Laser Scans. *Remote Sensing*, 13, 1369, doi:10.3390/rs13071369.
- Kerekes, G., Schwieger, V. (2020). Elementary Error Model Applied to Terrestrial Laser Scanning Measurements: Study Case Arch Dam Kops. *Mathematics*, Vol. 8, 593, doi:10.3390/math8040593.
- Kermarrec, G., Kargoll, B., Alkhatib, H. (2020). Deformation Analysis Using B-Spline Surface with Correlated Terrestrial Laser Scanner Observations—A Bridge Under Load. *Remote Sensing*, Vol. 12, 829, doi:10.3390/rs12050829.
- Koch, K. R. (2009). Fitting free-form surfaces to laserscan data by NURBS, In: *allgemeine vermessungs-nachrichten (avn)*, Vol. 116, No. 4, pp. 134–140.
- Liebig, J., Grünberg, J., Paffenholz, J.-A., Vennegeerts, H. (2011). Taktile und laserbasierte Messverfahren für die messtechnische Überwachung einer Autobahnbrücke. In: *Bautechnik*, Vol. 88, No. 11, pp. 749–756. doi: 10.1002/bate.201101514 2011.
- Medić, T., Kuhlmann, H., Holst, C. (2020). Designing and Evaluating a User-Oriented Calibration Field for the Target-Based Self-Calibration of Panoramic Terrestrial Laser Scanners. *Remote Sensing*, Vol. 12, 15, doi:10.3390/rs12010015.
- Mukupu, W., Roberts, G.W., Hancock, C.M., Al-Manasir, K. (2016). A review of the use of terrestrial laser scanning application for change detection and deformation monitoring of structures. *Survey Review*, 1–18, doi:10.1080/00396265.2015.1133039.
- Neuner, H., Holst, C., Kuhlmann, H. (2016). Overview on current modelling strategies of point clouds for deformation analysis. In: *allgemeine vermessungs-nachrichten (avn)*, Vol. 123, No. 1-12, pp. 328–339.
- Osada, E., Sośnica, K., Borkowski, A., Owczarek-Wesołowska, M., Gromczak, A. (2017). A Direct Georeferencing Method for Terrestrial Laser Scanning Using GNSS Data and the Vertical Deflection from Global Earth Gravity Models. *Sensors (Basel)*, 17, doi:10.3390/s17071489.
- Paffenholz, J.-A. (2012). Direct geo-referencing of 3D point clouds with 3D positioning sensors. PhD thesis. Munich : DGK (Reihe C, 689), doi: 10.15488/4698.
- Paffenholz, J.-A., Wujanz, D. (2019). Spatio-temporal monitoring of a bridge based on 3d point clouds - a comparison among several deformation measurement approaches. In: *Proceedings of the 4th Joint International Symposium on Deformation Monitoring (JISDM)*. Athens, Greece.
- Paulus, S. (2019). Measuring crops in 3D: using geometry for plant phenotyping. *Plant Methods*, 15, 103, doi:10.1186/s13007-019-0490-0.
- Peter, K.D., d'Oleire-Oltmanns, S., Ries, J.B., Marzloff, I., Ait Hssaine, A. (2014). Soil erosion in gully catchments affected by land-levelling measures in the Souss Basin, Morocco, analysed by rainfall simulation and UAV remote sensing data. *CATENA* 113, 24–40. doi:10.1016/j.catena.2013.09.004.
- Piegl, L., Tiller, W. (1997): *The NURBS Book*. Second Edition. Berlin, Heidelberg: Springer (Monographs in Visual Communication). doi: 10.1007/978-3-642-59223-2.
- Schill, F., Eichhorn, A. (2019). Deformation Monitoring of Railway Bridges with a Profile Laser Scanner. *zfv (Zeitschrift für Geodäsie, Geoinformation und Landmanagement)*, Vol. 144, No. 2, pp. 109-118, doi: 10.12902/zfv-0248-2018.

Schmitt, C., Neuner, H., Kromoser, B. (2019). Geodetic surface based methods for structural analysis during construction phase. In: Proceedings of the 4th Joint International Symposium on Deformation Monitoring (JISDM). Athens, Greece.

Steinhoff-Knopp, B., Eltner, A., Hake, F., Paffenholz, J.-A. (2019): Methoden zur skalenübergreifend hochaufgelösten Erfassung und Quantifizierung von Bodenerosion durch Wasser. In: Alkhatib, H. und Paffenholz, J.-A. (Hg.): Tagungsband GeoMonitoring 2019. Hannover, S. 75–89. doi: 10.15488/4514.

Truong-Hong, L., Lindenbergh, R. (2019): Measuring deformation of bridge structures using laser scanning data. In: Proceedings of the 4th Joint International Symposium on Deformation Monitoring (JISDM). Athens, Greece.

Uggla, G., Horemuz, M. (2021). Conceptualizing Georeferencing for Terrestrial Laser Scanning and Improving Point Cloud Metadata. *Journal of Surveying Engineering*, Vol. 147, 2520001, doi:10.1061/(ASCE)SU.1943-5428.0000344.

Wujanz, D., Burger, M., Mettenleiter, M., Neitzel, F. (2017). An intensity-based stochastic model for terrestrial laser scanners. In: *ISPRS Journal of Photogrammetry and Remote Sensing*, Vol. 125, pp. 146-155, doi: 10.1016/j.isprsjprs.2016.12.006.

Wujanz, D., Burger, M., Tschirschwitz, F., Nietzschmann, T., Neitzel, F., Kersten, T. P. (2018). Determination of Intensity-Based Stochastic Models for Terrestrial Laser Scanners Utilising 3D-Point Clouds. In: *Sensors (Basel)* 18 (7). DOI: 10.3390/s18072187.

Wunderlich, T., Niemeier, W., Wujanz, D., Holst, C., Neitzel, F., Kuhlmann, H (2016). Areal deformation analysis from TLS point clouds – the challenge. In: *allgemeine vermessungs-nachrichten (avn)*, Vol. 123, No. 11-12, pp. 340–351.

Ziamtsov, I., Navlakha, S. (2020). Plant 3D (P3D): a plant phenotyping toolkit for 3D point clouds. *Bioinformatics*, 36, 3949–3950, doi:10.1093/bioinformatics/btaa220.

## BIOGRAPHICAL NOTES

**Prof. Dr.-Ing. Jens-André Paffenholz** received his diploma (Dipl.-Ing.) and his Ph.D. in Geodesy and Geoinformatics at the Leibniz University Hannover in 2006 and 2012, respectively. From 02-2014 to 11-2019, he has been postdoctoral fellow and the leader of the working group Terrestrial Laser Scanner Based Multi-Sensor Systems | Engineering Geodesy at the Geodetic Institute of the Leibniz University Hannover. Since 11-2019 he is a full professor for Geomatics for underground systems at the Institute of Geo-Engineering of Clausthal University of Technology. His research profile is based on laser scanning and multi-sensor systems with the aim of an efficient three-dimensional data acquisition for monitoring and change detection of natural and anthropogenic structures. He is active in national (DVW e. V. WG 4: "Engineering Surveys") and international scientific associations (working group chair of IAG WG 4.1.3: "3D Point Cloud based Spatio-temporal Monitoring").

**Dr. Corinna Harmening** received her Master degree in Geodesy and Geoinformatics at Leibniz University Hanover in 2013. She received her Ph.D. from TU Wien in 2020. Currently, she is a postdoctoral fellow at the department for geodesy and geoinformation at TU Wien. She is active in international scientific associations (working group co-chair of IAG WG 4.1.3: "3D Point Cloud based Spatio-temporal Monitoring" and commission co-chair of FIG Commission 6: "Engineering Surveys").

**Dr. Bastian Steinhoff-Knopp** studied geography, geology, geoinformatics and cartography at the Leibniz Universität Hannover and obtained his PhD in natural sciences in 2016. He has been

working since 2011 at the Institute for Physical Geography and Landscape Ecology at the Leibniz Universität Hannover, Germany. His main research interests are the understanding of spatial and temporal patterns of soil erosion under different management practices, the development of field methods to estimate soil loss and the assessment and mapping of regulating ecosystem services.

## CONTACTS

Prof. Dr.-Ing. Jens-André Paffenholz  
Clausthal University of Technology  
Institute of Geo-Engineering  
Chair of Geomatics for Underground Systems  
Erzstraße 18, 38678 Clausthal-Zellerfeld, GERMANY  
jens-andre.paffenholz@tu-clausthal.de  
www.ige.tu-clausthal.de

Dr. Corinna Harmening  
TU Wien  
Department of Geodesy and Geoinformation  
Wiedner Hauptstr. 8/E120, 1040 Vienna, AUSTRIA  
corinna.harmening@geo.tuwien.ac.at  
www.geo.tuwien.ac.at

Dr. Bastian Steinhoff-Knopp  
Leibniz University Hannover  
Institute of Physical Geography & Landscape Ecology  
Schneiderberg 50, 30167 Hannover, Germany  
steinhoff-knopp@phygeo.uni-hannover.de  
www.phygeo.uni-hannover.de